MS.ID-IJPBS-9779
International Journal of Pharmacy and Biological Sciences-IJPBS™ (2026) 16 (4): 68-80
Online ISSN: 2230-7605, Print ISSN: 2321-3272
Research Article | Pharmaceutical Sciences | OA Journal | MCI Approved | Index Copernicus

Green Synthesis, Central Composite Design-Based Optimization and Evaluation of Cerium Oxide Nanoparticle-Loaded Gel Using *Punica granatum* Peel Extract for Topical Antioxidant Application

J Adlin Jino Nesalin, Ganesh N S, and Druti S N*

Department of Pharmaceutics, T. John College of Pharmacy, Rajiv Gandhi University of Health Sciences, Bangalore, Karnataka, India.

Received: 23 May 2026/ Accepted: 8 Jun 2026 / Published online: 1 Oct 2026
***Corresponding Author Email:** druti123@gmail.com

Abstract

The present study was undertaken to synthesize, statistically optimize, characterize and formulate a Cerium oxide nanoparticle-loaded gel using Punica granatum (pomegranate) peel extract for topical antioxidant application. Cerium oxide nanoparticles (CeO_2 NPs) possess excellent antioxidant, free-radical-scavenging, anti-inflammatory and wound-healing properties owing to the reversible Ce^{3+}/Ce^{4+} redox couple on their surface, but their therapeutic performance depends on colloidal stability and efficient topical delivery. CeO_2 nanoparticles were synthesized by a green precipitation route using Cerium nitrate hexahydrate as the precursor and pomegranate peel extract as a natural reducing and capping agent. A two-factor, two-level Central Composite Design (CCD) was employed using Design-Expert® software (Version 12, Stat-Ease Inc.) to study the influence of CeO_2 nanoparticle concentration (0.25–0.75 g) and pomegranate peel extract concentration (5–15 mL) on antioxidant activity (R1) and drug content (R2), generating thirteen experimental runs. Drug–excipient compatibility was confirmed by FTIR, while DSC and XRD verified thermal stability and crystallinity. Among the thirteen suspensions, F2 exhibited the highest antioxidant activity (91.67 ± 0.38%) and drug content (94.89 ± 0.37%). The design-optimized formulation (F14) was incorporated into a Carbopol 934 gel base and characterized by SEM, particle size and zeta potential analysis, showing predominantly spherical to quasi-spherical particles of average size 56.3 nm, PDI 0.213 and zeta potential +28.4 mV. The optimized gel exhibited pH 6.33 ± 0.02, viscosity 3278 ± 1.63 cP, spreadability 6.7 ± 0.16 g·cm/s, antioxidant activity 85.06 ± 0.15% and drug content 96.47 ± 1.91%, with a cumulative *in vitro* release of 82.72 ± 0.05% at 8 hours that best fitted the Korsmeyer–Peppas model ($r^2 = 0.9966$, $n = 0.7260$), indicating non-Fickian (anomalous) release. The study demonstrates that a green-synthesized, CCD-optimized cerium oxide nanoparticle gel is a stable, biocompatible and effective topical antioxidant system with potential application in the management of oxidative-stress-related skin disorders and wound healing.

Keywords

Cerium oxide nanoparticles, green synthesis, *Punica granatum*, Central Composite Design, Antioxidant activity.

*****

INTRODUCTION:

Nanotechnology involves the design, synthesis and application of materials at the nanometre scale (1–1000 nm), a size regime in which physicochemical properties differ markedly from the corresponding bulk material[1]. This departure from bulk behaviour has enabled the use of nanomaterials across electronics, energy, textiles and, most prominently, the biomedical sciences, where nanotechnology has enabled drug-delivery systems capable of precise targeting, controlled release and improved bioavailability while limiting systemic adverse effects[2].

Nanoparticles are among the most versatile of these carrier systems. Their size, surface charge and composition can be tuned to achieve a desired pharmacokinetic and pharmacodynamic profile, and they are broadly classified as organic, inorganic or carbon-based, each offering distinct structural and functional advantages[3]. Among the inorganic nanomaterials, metal-oxide nanoparticles such as cerium oxide (CeO_2), zinc oxide and titanium dioxide have drawn particular interest for topical and dermatological use because of their intrinsic physicochemical activity and comparatively favourable safety profile on intact skin[4,5].

Topical drug delivery, in which an active agent is applied directly to the skin, offers a route for localized therapy while avoiding first-pass metabolism and improving patient compliance[6]. However, the stratum corneum presents a formidable barrier to permeation of most therapeutic molecules, and nanoparticulate carriers are increasingly used to improve deposition and residence of actives within the epidermal layers while enabling sustained release[7].

Oxidative stress arising from excess reactive oxygen species (ROS) is a central contributor to photo ageing, inflammation, delayed wound healing and a range of chronic dermatological conditions[8]. Cerium oxide nanoparticles are unique among metal-oxide nanomaterials in that cerium can reversibly switch between the Ce^{3+} and Ce^{4+} oxidation states on the nanoparticle surface[9]. This redox couple allows CeO_2 nanoparticles to mimic the catalytic activity of endogenous antioxidant enzymes such as superoxide dismutase and catalase, enabling them to repeatedly scavenge superoxide and other free radicals without being consumed in the reaction[10]. This "regenerative" antioxidant behaviour, combined with a fluorite cubic crystal structure that confers excellent thermal and chemical stability, has made nano-ceria an attractive candidate for topical antioxidant and wound-healing formulations[11].

The efficacy and safety of metal-oxide nanoparticles for topical use can be further improved by employing green, plant-mediated synthesis routes in place of conventional chemical reduction methods, which often rely on hazardous reducing and capping agents[12,13]. *Punica granatum* (pomegranate), particularly its peel, is a rich source of polyphenols, flavonoids, tannins and ellagitannins such as punicalagin, which possess pronounced antioxidant, anti-inflammatory and wound-healing activity[14]. When used in the green synthesis of CeO_2 nanoparticles, pomegranate peel extract serves a dual role: its phytoconstituents act as natural reducing and capping agents that control nanoparticle nucleation and growth, while contributing an intrinsic antioxidant activity that is complementary to that of the ceria surface itself[15,16]. Building on this rationale, the present study was designed to synthesize cerium oxide nanoparticles by a green precipitation method using Punica granatum peel extract, to statistically optimize the concentrations of cerium oxide nanoparticle and pomegranate peel extract using a Central Composite Design (Design of Experiments, DOE) with antioxidant activity and drug content as the responses, to characterize the optimized nanoparticles by SEM, particle size, zeta potential, FTIR, DSC and XRD, and to incorporate the optimized nanoparticle suspension into a Carbopol 934 gel base for evaluation of its physicochemical, antioxidant and *in vitro* release performance as a topical antioxidant delivery system.

MATERIALS AND METHODOLOGY:

Chemicals and Reagents:

Cerium nitrate hexahydrate [$Ce(NO_3)_3 \cdot 6H_2O$, molecular weight 434.22 g/mol] was used as the cerium precursor. Carbopol 934 served as the gelling agent, propylene glycol as a humectant/co-solvent, Tween 80 as a surfactant, glycerin as an emollient, triethanolamine as a neutralizing and pH-adjusting agent, and methyl paraben as a preservative. 2,2-Diphenyl-1-picrylhydrazyl (DPPH) was used as the free-radical reagent for the antioxidant assay. All chemicals and reagents used were of analytical or pharmaceutical grade, procured from standard commercial suppliers (Otto-Kemi, Mumbai; Karnataka Fine Chem., Bengaluru; Techno Lab Kraft, Mumbai; Fisher Scientific, Mumbai; and Sigma-Aldrich Chemicals Pvt. Ltd., Bengaluru)[17].

Instruments:

The major instruments employed included an electronic analytical balance (Citizen Scales Pvt. Ltd., Mumbai), a UV-Visible spectrophotometer (Shimadzu UV-1800, Japan), an FT-IR

spectrophotometer (Shimadzu IR-Affinity-1, Japan), a magnetic stirrer (Remi Elektrotechnik Ltd., Vasai), a centrifuge (Remi Elektrotechnik Ltd., Vasai), a differential scanning calorimeter (Perkin-Elmer 4000 series), an X-ray diffractometer (Bruker AXS D8 Advance, Germany), a scanning electron microscope (Hitachi SU 3500), a Zetasizer (Malvern Instruments, Nano ZS90) and a Brookfield rotational viscometer[18,19].

Pre-formulation Studies:

Solubility: The solubility of cerium oxide was determined in distilled water, ethanol, concentrated hydrochloric acid, propylene glycol, and phosphate buffers of pH 5.4 and 6.8 by shake-flask equilibration, since CeO_2 is a highly refractory oxide whose dissolution is strongly dependent on particle size and thermal history.

Determination of λ max: As CeO_2 is insoluble in most solvents, a dispersion (~100 µg/mL) was prepared by wetting ~10 mg of nano-CeO_2 powder with ethanol and making up the volume with ethanol–water (50:50 v/v) containing 0.05% polysorbate-80, followed by probe-sonication for 10 min. The dispersion was scanned on a Shimadzu UV-1800 spectrophotometer between 200–600 nm against a solvent blank to locate the characteristic absorption maximum[20].

Calibration curve: A primary stock (1 mg/mL) of CeO_2 in phosphate buffer pH 5.4 was prepared with the aid of 0.05% w/v Tween-80 and sonication, diluted to a secondary stock (100 µg/mL), and further diluted to working standards of 2, 4, 6, 8 and 10 µg/mL. Absorbance of each standard was measured in triplicate at λmax using 1 cm quartz cuvettes, and a calibration curve of absorbance versus concentration was constructed.

FT-IR spectroscopy: Drug–excipient compatibility was evaluated by triturating cerium oxide, cerium nitrate hexahydrate and Carbopol 934, individually and as a physical mixture, with potassium bromide and compressing the mixture into transparent pellets under hydraulic pressure. Pellets were scanned between 4000–400 cm^{-1} on a Shimadzu FT-IR spectrophotometer to identify characteristic functional-group peaks and rule out incompatibility.

Differential scanning calorimetry (DSC): Cerium oxide powder was dried at 100–110°C for 1 h to remove adsorbed moisture, sealed in alumina pans, and heated from 25°C to 800–1000°C at 10°C/min under a nitrogen purge (50 mL/min) using an empty alumina pan as reference, to assess thermal stability, dehydration, and decomposition of residual precursor.

X-ray diffraction (XRD): The crystalline nature and phase purity of cerium oxide were examined using Cu-Kα radiation (λ = 1.5406 Å) at 40 kV and 40 mA, scanning over a 2θ range of 5–90° at a step width of 1.0° min^{-1}.

Green Synthesis of Cerium Oxide Nanoparticles:

Preparation of pomegranate peel extract: Fresh pomegranate (*Punica granatum*) peels were washed thoroughly with distilled water and air-dried for 3–5 days, or oven-dried at 50°C until crisp, and then ground to a fine powder. Ten grams of the dried peel powder were added to 100 mL of distilled water and heated at 60°C for 30 minutes with constant stirring. The extract was filtered through muslin cloth/Whatman filter paper and stored at 4°C for use as the reducing and stabilizing agent[21].

Synthesis of cerium oxide nanoparticles: 50 ml of 1 mM cerium nitrate hexahydrate solution were mixed with 50 ml of the freshly prepared pomegranate peel extract in a beaker and heated at 60–80°C for 2–3 hours under constant stirring. A gradual colour change in the reaction mixture, indicative of nanoparticle formation, was observed. The mixture was then cooled to room temperature, centrifuged at 10,000 rpm for 15 minutes, and the pellet obtained was washed sequentially with deionized water and ethanol to remove unreacted precursor and organic residues, and finally dried at 80°C to yield cerium oxide nanoparticle powder[22].

Preparation of Cerium Oxide Nanoparticle-Loaded Gel:

The cerium oxide nanoparticle-loaded gel was prepared by the direct dispersion method. Carbopol 934 (0.10 g) was slowly dispersed in a small quantity of distilled water under continuous stirring and allowed to hydrate for 2–3 hours to obtain the gel base. In a separate beaker, cerium oxide nanoparticles were dispersed in propylene glycol (1 mL) and Tween 80 (0.10 mL); to this, pomegranate peel extract, Glycerin (0.5 mL) and methyl paraben (0.02 g) were added and mixed thoroughly using a magnetic stirrer. This nanoparticle dispersion was then slowly incorporated into the hydrated Carbopol gel base under continuous stirring, and the pH was adjusted with triethanolamine to obtain a homogeneous, skin-compatible gel[23].

Experimental Design (DOE):

A Central Composite Design (CCD), a response-surface methodology, was employed to study and optimize the effect of two independent formulation variables — cerium oxide nanoparticle concentration (Factor A) and pomegranate peel extract concentration (Factor B) — on two dependent responses, namely antioxidant activity (R1) and drug content (R2), of the cerium oxide nanoparticle suspension. A commercially available statistical software package (Design-Expert®, Version 12, Stat-

Ease Inc., Minneapolis, MN, USA) was used for design generation and statistical analysis. CCD evaluates the interaction between the factors at all possible combinations and, with the inclusion of axial and centre points, generated a total of thirteen experimental runs, the order of which was randomized to minimize the influence of uncontrolled variables. Analysis of variance (ANOVA) was subsequently applied to assess the significance of the fitted quadratic models and of the individual formulation variables[24].

Table 1: Independent and dependent variables in the Central Composite Design

Independent variable	Low level	High level
A: Cerium oxide nanoparticle (g)	0.25	0.75
B: Pomegranate peel extract (mL)	5	15

Dependent variables: R1 – Antioxidant activity (%); R2 – Drug content (%)

Table 2: Central Composite Design matrix for cerium oxide nanoparticle suspension (F1–F13)

Std	Run	Factor A: CeO_2 NP (g)	Factor B: PPE (mL)
5	1	0.146	10
8	2	0.5	17.07
3	3	0.25	15
12	4	0.5	10
1	5	0.25	5
4	6	0.75	15
9	7	0.5	10
2	8	0.75	5
11	9	0.5	10
10	10	0.5	10
13	11	0.5	10
6	12	0.854	10
7	13	0.5	2.93

Evaluation of Cerium Oxide Nanoparticles:

Antioxidant activity (DPPH assay): A 0.1 mM DPPH solution was prepared in methanol and protected from light. One millilitre of each nanoparticle suspension (F1–F13) was mixed with 3 mL of DPPH solution, vortexed and incubated in the dark for 30 minutes at room temperature, after which absorbance was measured at 517 nm.

Percentage inhibition was calculated as:

$$\% \text{ Inhibition} = \frac{(A\ control - A\ sample)}{A\ control} \times 100.$$

Drug content: 1 ml of each suspension was made up to 10 mL with phosphate buffer pH 5.4, filtered, and analysed by UV spectrophotometry at 320 nm against a calibration curve.

Scanning electron microscopy (SEM): Surface morphology was examined by diluting the nanoparticle dispersion with ultrapure water (1:5), depositing a drop on an aluminium stub, vacuum-drying, and imaging at 15 kV.

Zeta potential and particle size: Particle size, polydispersity index (PDI) and zeta potential were determined using a Zetasizer (dynamic light scattering) after suitable dilution of the formulation with phosphate buffer (pH 7.4).

Post-Formulation Evaluation of the Nanoparticle-Loaded Gel:

Physical appearance: The prepared gel was inspected visually for colour, odour, homogeneity, texture and washability.

pH: Measured using a calibrated digital pH meter with the electrode immersed directly in the gel, in triplicate.

Viscosity: Determined using a Brookfield viscometer; the gel was allowed to equilibrate for 30 min at 23 ± 1°C, and the spindle was rotated at 50 rpm for 10 min, with measurements performed in triplicate.

Spreadability: Determined by placing 1 g of gel within a 2 cm diameter circle marked on a glass plate, sandwiching with a second plate, applying a 500 g weight for 1 min, and measuring the diameter of spread; Spreadability (S) = M × L / T, where M is the weight tied to the upper slide, L is the length moved by the slide, and T is the time taken.

Stability studies: The optimized gel was stored at room temperature and under accelerated conditions (37 ± 2°C, 75 ± 5% RH) and periodically inspected for phase separation, colour change and consistency.

***In vitro* drug release and kinetics:** Release of cerium oxide from the optimized gel was studied using a

dissolution apparatus in phosphate buffer (pH 5.4) over 480 minutes, with samples withdrawn at fixed intervals and analysed by UV spectrophotometry. The cumulative release data were fitted to zero-order, first-order, Higuchi and Korsmeyer–Peppas kinetic models to elucidate the release mechanism.

RESULTS AND DISCUSSION:

Cerium oxide was obtained as a pale-yellow, amorphous powder, consistent with the reported appearance of the drug. Solubility studies showed that cerium oxide was very soluble in concentrated hydrochloric acid, sparingly soluble in distilled water, slightly soluble in phosphate buffer at pH 5.4 and 6.8, dispersible in propylene glycol and insoluble in ethanol, a pattern consistent with the highly refractory nature of the CeO_2 lattice and its slow dissolution outside strongly acidic media.

UV spectrophotometric analysis revealed λmax at 320 nm, consistent with the reported standard range of 310-340 nm for Cerium oxide, confirming its identity **(Table 1, Fig 1)**.

Table 1: Determination of λ_{max} of Cerium oxide

Compound	Observed λ_{max} (nm)	Standard range (nm)
Cerium oxide	320	310-340

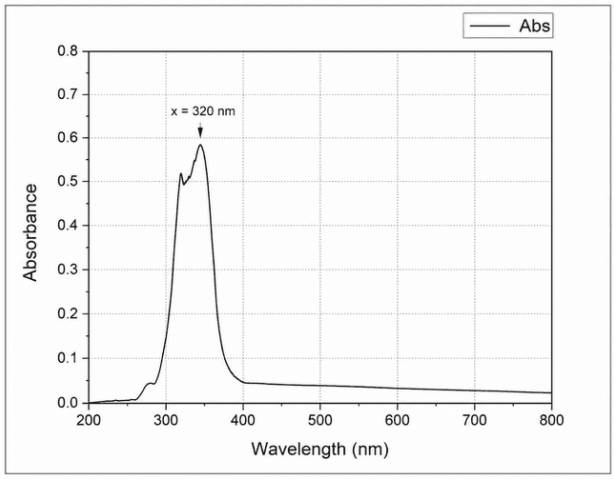


Fig 1: UV-Visible absorption spectrum of Cerium oxide

The calibration curve of Cerium oxide in phosphate buffer pH 5.4 exhibited a linear relationship between absorbance and concentration over the range of 0-10 µg/mL, following Beer-Lambert's law, with a correlation coefficient (r^2) of 0.9916, confirming the linearity and reproducibility of the method **(Table 2)**.

Table 2: Calibration curve data of Cerium oxide in phosphate buffer pH 5.4

Concentration (µg/mL)	Absorbance (mean ± SD, n = 3)
0	0
2	0.23 ± 0.011
4	0.37 ± 0.018
6	0.50 ± 0.007
8	0.65 ± 0.025
10	0.80 ± 0.007

FT-IR analysis of Cerium oxide showed characteristic bands corresponding to O-H stretching, H-O-H bending, residual carbonate/precursor vibrations, and the Ce-O stretch, confirming its identity **(Table 3, Fig 2)**

Table 3: FTIR spectral values of Cerium oxide

Functional group	Standard range (cm^{-1})	Observed peak (cm^{-1})
O-H stretch	3200-3600	3432
H-O-H bending	1600-1650	1631
Carbonate/precursor residues	1350-1500	1475
Ce-O stretch	400-600	545

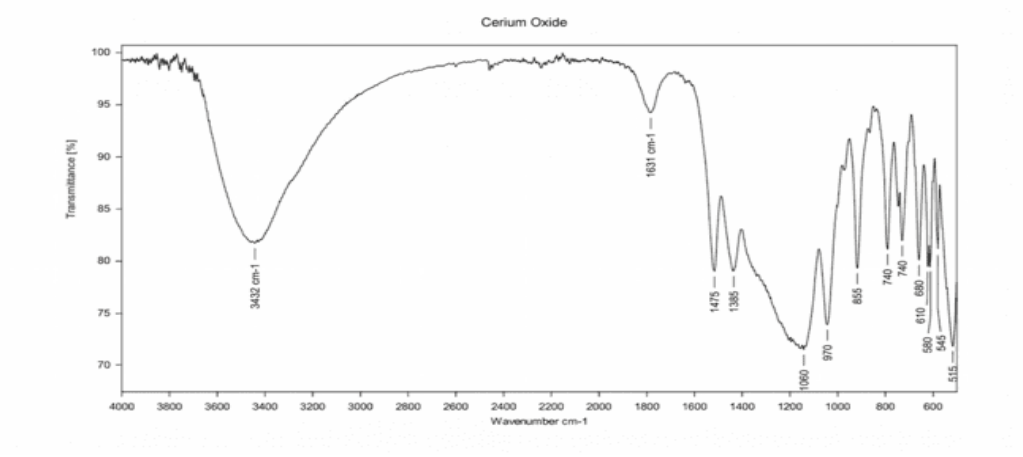


Fig 3: FTIR spectrum of Cerium oxide

DSC analysis of Cerium oxide showed good thermal stability at elevated temperature with minimal phase change, consistent with its stable cubic fluorite crystal structure **(Fig 4)**. X-ray diffraction confirmed a well-defined crystalline pattern characteristic of the cubic fluorite phase of Cerium oxide **(Fig 5)**.

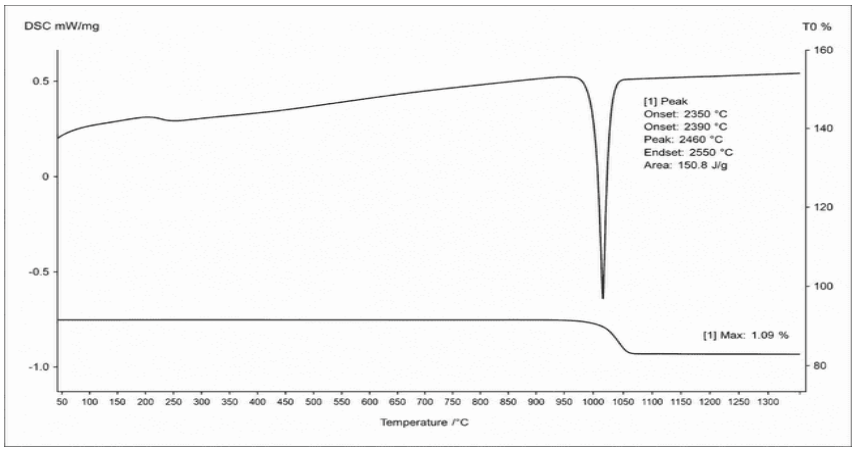


Fig 4: DSC thermogram of Cerium oxide

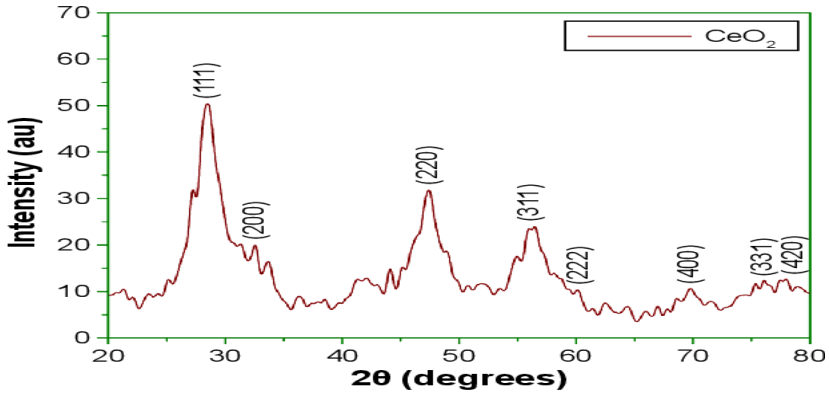


Fig 5: XRD pattern of Cerium oxide

Characterization of Cerium Oxide Nanoparticles

The green-synthesized Cerium oxide nanoparticles appeared as a pale-yellow fine powder **(Fig 6)**. Morphological analysis by scanning electron microscopy revealed near-spherical, well-dispersed nanoparticles **(Fig 7)**. Zeta potential measurement showed a value of -21.5 mV **(Fig 8)**, indicating a moderately stable dispersion with adequate electrostatic repulsion between particles. Particle size analysis showed an average diameter of 131.5 nm **(Fig 9,10,11)**, confirming successful nanoscale

synthesis and supporting suitable spreadability of the nanoparticle-loaded gel.

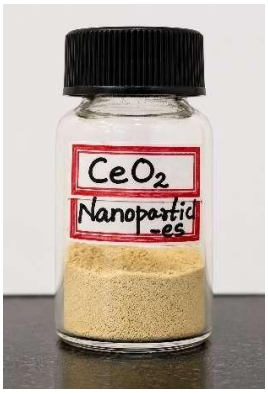


Fig 6: Green-synthesized Cerium oxide nanoparticles

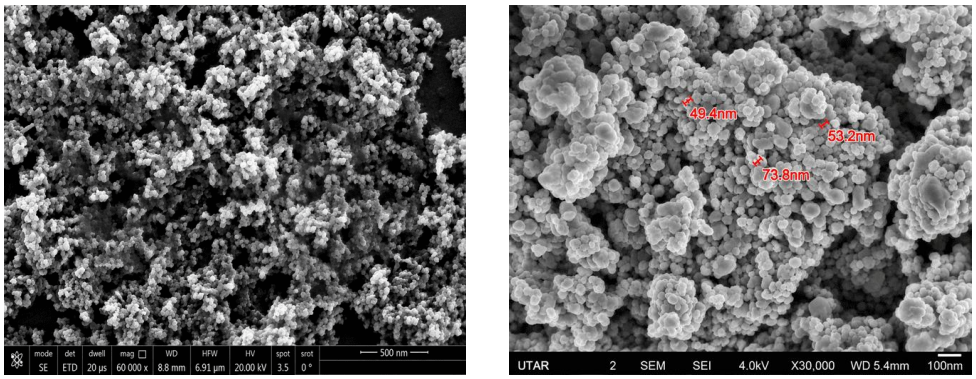
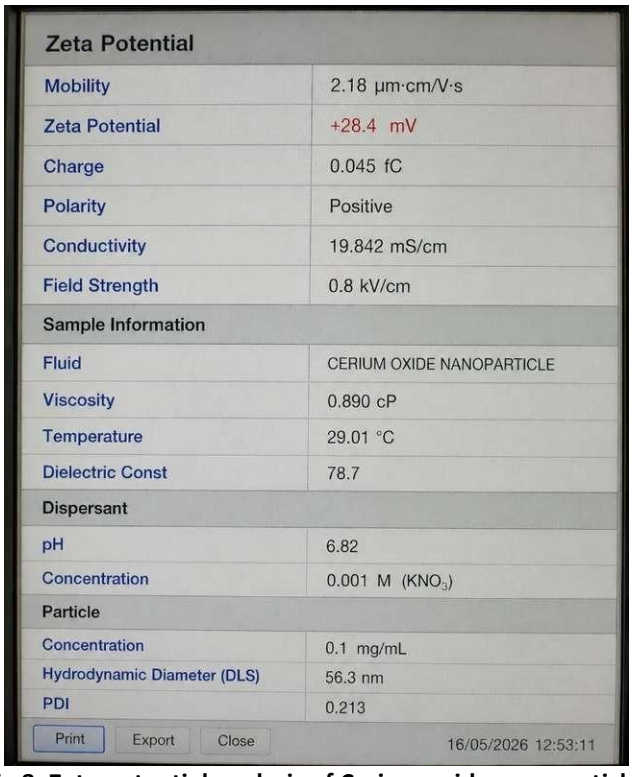


Fig 7: SEM images of Cerium oxide nanoparticles



Zeta Potential	
Mobility	2.18 µm·cm/V·s
Zeta Potential	+28.4 mV
Charge	0.045 fC
Polarity	Positive
Conductivity	19.842 mS/cm
Field Strength	0.8 kV/cm
Sample Information	
Fluid	CERIUM OXIDE NANOPARTICLE
Viscosity	0.890 cP
Temperature	29.01 °C
Dielectric Const	78.7
Dispersant	
pH	6.82
Concentration	0.001 M (KNO_3)
Particle	
Concentration	0.1 mg/mL
Hydrodynamic Diameter (DLS)	56.3 nm
PDI	0.213

Print Export Close 16/05/2026 12:53:11

Fig 8: Zeta potential analysis of Cerium oxide nanoparticles

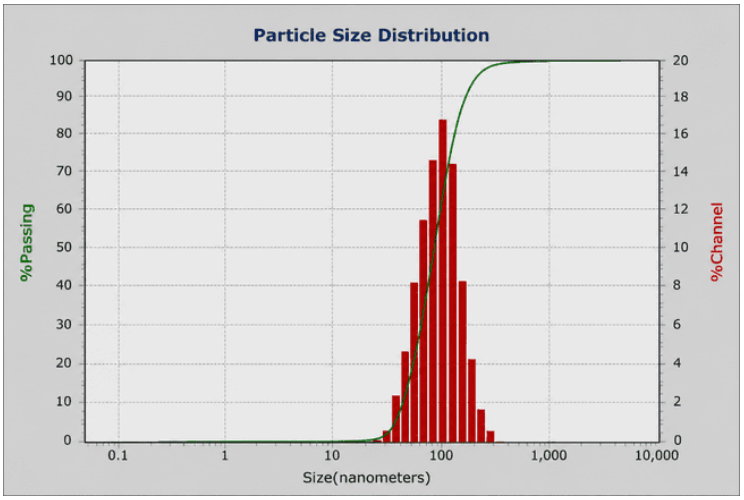


Fig 9: Particle size distribution of Cerium oxide nanoparticles

Peaks Summary		
Dia(nm)	Vol%	Width
98.7	100	72.4

Fig 10: Peak Summary of Particle size

Percentiles	
%Tile	Size(nm)
10.00	91.80
20.00	105.0
30.00	115.3
40.00	124.9
50.00	134.5
60.00	145.0
70.00	157.5
80.00	174.2
90.00	202.2
95.00	231.4

Title	
Particle Size Analysis	
Identifiers	
CERIUM OXIDE	
Database Record	84
Run Number	1 of 1
Date	16/05/2026
Time	12:53
Acquired Date	16/05/2026
Acquired Time	12:53
Serial Number	W32331
Calculated Data	
Above Residual	0
Below Residual	0
Loading Index	9.147
Conc. Index	15.67
RMS Residual	0.091%
Cell Temp (C)	29.01
Viscosity(c p)	0.8900
Reflected Pw (uW)	1.82
Recalculation Status	
Live-Meas: Original	

Fig 11: Particle size analysis

Thirteen cerium oxide nanoparticle suspensions (F1–F13) were prepared according to the Central Composite Design matrix by varying the concentrations of cerium oxide nanoparticle (0.25–0.75 g) and pomegranate peel extract (5–15 mL). The percentage antioxidant activity of the suspensions, determined by the DPPH radical-scavenging assay, ranged from 70.27 ± 0.17% (F1) to 91.67 ± 0.38% (F2), while the percentage drug content ranged from 78.47 ± 0.28% (F1) to 94.89 ± 0.37% (F2). Both responses were lowest at the low-CeO_2/low-PPE axial and factorial combinations and increased toward the centre and upper factorial points, with formulation F2 (0.5 g CeO_2 NP, 17.07 mL PPE)

consistently providing the highest antioxidant activity and drug content among all thirteen runs, indicating that a moderate-to-high nanoparticle load combined with a comparatively high extract concentration favoured both free-radical scavenging capacity and nanoparticle loading efficiency **(Table 4).**

Table 4: Observed responses in the Central Composite Design for cerium oxide nanoparticle suspension (F1–F13)

Std	Run	Factor A: CeO_2 NP (g)	Factor B: PPE (mL)	R1: Antioxidant (%)	R2: Drug content (%)
5	1	0.146	10	70.27	78.47
8	2	0.5	17.07	91.67	94.89
3	3	0.25	15	78.35	86.73
12	4	0.5	10	80.16	83.64
1	5	0.25	5	75.92	79.83
4	6	0.75	15	84.58	90.67
9	7	0.5	10	88.64	91.54
2	8	0.75	5	84.35	89.75
11	9	0.5	10	89.62	89.75
10	10	0.5	10	87.83	89.00
13	11	0.5	10	82.97	85.23
6	12	0.854	10	82.11	88.65
7	13	0.5	2.93	74.79	78.64

Analysis of variance (ANOVA) performed on the quadratic models fitted to both responses confirmed the statistical adequacy of the Central Composite Design. For antioxidant activity, the model F-value of 3.99 ($p = 0.0495$) indicated a statistically significant model, with the linear term for CeO_2 nanoparticle concentration (A) and its quadratic term (A^2) identified as significant contributors ($p < 0.05$), while the effect of pomegranate peel extract concentration (B) approached significance ($p = 0.0625$). For drug content, the model F-value of 4.33 ($p = 0.0408$) likewise indicated significance, with both the CeO_2 nanoparticle concentration (A, $p = 0.0022$) and pomegranate peel extract concentration (B, $p = 0.0150$) emerging as significant linear terms. In both models, the lack-of-fit F-values (1.18 and 0.95, respectively) were non-significant relative to pure error, confirming that the quadratic models adequately described the experimental data without unexplained systematic deviation. The corresponding contour and three-dimensional response-surface plots showed smooth, concentric contours for both responses, with antioxidant activity and drug content increasing steadily with rising CeO_2 nanoparticle concentration and moderate-to-high pomegranate peel extract levels, reaching a central peak of approximately 85.8% antioxidant activity and 94.9% drug content at the optimum combination of both factors, before declining slightly at extreme factor levels — a trend attributable to saturation of the reducing capacity of the extract and possible aggregation or reduced encapsulation efficiency of the nanoparticles at very high loadings**.(Fig 12,13).**

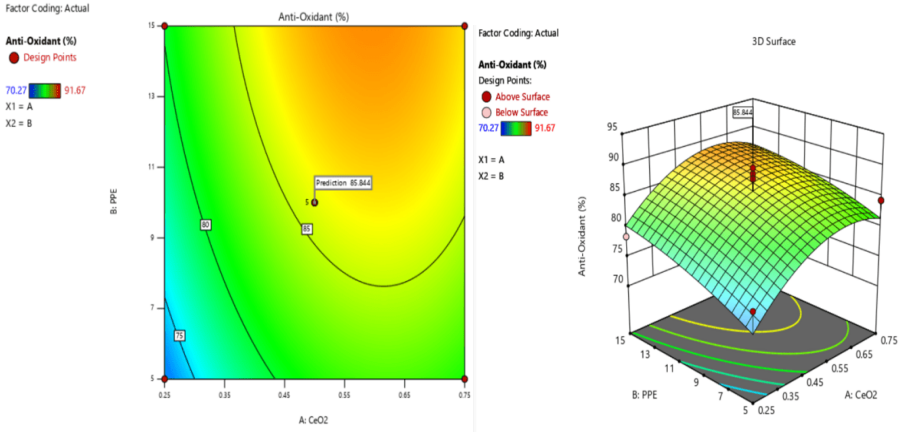


Fig 12: Percentage Anti-Oxidant Activity, 3D surfaces of percentage Anti-Oxidant Activity

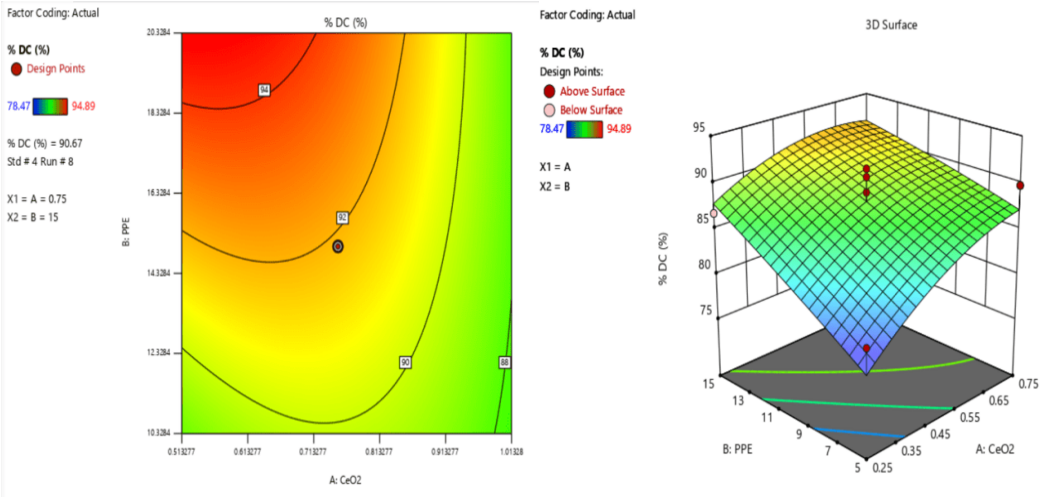


Fig13: Percentage Drug Content, 3D surfaces of percentage Drug Content

Using the desirability-based numerical optimization module of Design-Expert software, with antioxidant activity and drug content set to be maximized within the studied factor ranges, an optimized batch (F14) was derived and prepared at the design-recommended combination of cerium oxide nanoparticle and pomegranate peel extract concentrations. Scanning electron microscopy of the optimized nanoparticles revealed predominantly spherical to quasi-spherical particles with slight agglomeration, consistent with typical green-synthesized metal-oxide nanoparticles capped by plant polyphenols. Particle size analysis by dynamic light scattering showed an average particle diameter of 56.3 nm with a polydispersity index (PDI) of 0.213, indicating a fairly narrow and uniform nanoscale size distribution, while zeta potential measurement gave a value of +28.4 mV. A zeta potential of this magnitude, well above the conventional ± 25–30 mV threshold associated with electrostatically stabilized colloids, is indicative of good colloidal stability and a low tendency toward particle aggregation, consistent with capping of the nanoparticle surface by cationic or protonatable phytoconstituents of the pomegranate peel extract **(Fig 14).**

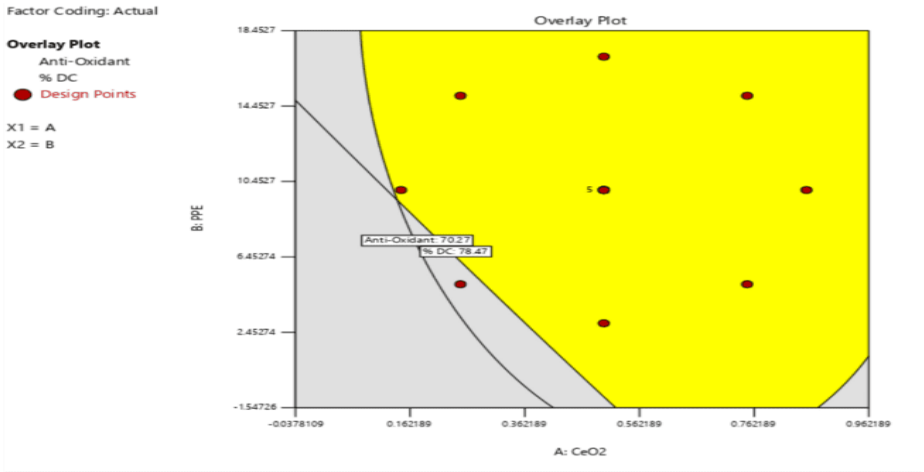


Fig 14: Graphical Optimization of Cerium Oxide Nanoparticles suspension

The optimized cerium oxide nanoparticle suspension (F14) was incorporated into a Carbopol 934 gel base by the direct dispersion method and evaluated for antioxidant activity and drug content, which were found to be 85.06 ± 0.15% and 96.47 ± 1.91% respectively — values that were comparable to, and for drug content even marginally higher than, the corresponding values for the nanoparticle suspension alone, indicating that gel incorporation did not compromise, and may have slightly improved apparent recovery of, the antioxidant and drug-loading performance of the nanoparticles **(Fig 12, Table 5).**



Fig 12: Optimized Cerium Oxide Nanoparticle Loaded Gel

Table 5: Physicochemical characteristics of the optimized cerium oxide nanoparticle-loaded gel (F14)

Parameter	Observation / Value (Mean ± SD, n = 3)
Colour	Off-white to pale yellow
Odour	Odourless
Texture / State	Smooth, semisolid
Washability	Easily washable
pH	6.33 ± 0.02
Viscosity (cP)	3278 ± 1.63
Spreadability (g·cm/s)	6.7 ± 0.16
Antioxidant activity (%)	85.06 ± 0.15
Drug content (%)	96.47 ± 1.91
Particle size (nm)	56.3
PDI	0.213
Zeta potential (mV)	+28.4

The prepared gel was off-white to pale yellow, odourless, smooth and semisolid in consistency, with good washability, all of which are desirable attributes for a cosmetically acceptable topical formulation. Its pH of 6.33 ± 0.02 lies close to the physiological pH of the skin surface, minimizing the likelihood of irritation on repeated topical application. The measured viscosity of 3278 ± 1.63 cP is consistent with a semisolid gel of adequate consistency for application without being excessively stiff, while the spreadability of 6.7 ± 0.16 g·cm/s indicates that the gel could be spread readily and uniformly over the skin surface with minimal shear, an important attribute for patient acceptability and dosing uniformity. Under both room-temperature and accelerated storage conditions (37 ± 2°C, 75 ± 5% RH), the optimized gel remained physically stable, with no phase separation, syneresis or change in colour or consistency observed, indicating that the Carbopol-based gel network adequately entrapped the nanoparticle dispersion without destabilization.

In vitro release studies of the optimized gel in phosphate buffer pH 5.4 demonstrated a gradual, sustained release profile, with cumulative release increasing from 7.88 ± 0.11% at 30 minutes to 82.72 ± 0.05% at the end of 480 minutes (8 hours). This progressive, non-burst release pattern is consistent with a diffusion-controlled release mechanism from the cross-linked Carbopol matrix, in which the nanoparticles must first diffuse through the hydrated polymer network before reaching the release medium. When the release data were fitted to the standard kinetic models, the correlation coefficients obtained were $r^2 = 0.9921$ for the zero-order model, $r^2 = 0.8915$ for the first-order model, $r^2 = 0.9499$ for the Higuchi model, and $r^2 = 0.9966$ for the Korsmeyer–Peppas model, with the latter yielding a release exponent (n) of 0.7260. The Korsmeyer–Peppas model provided the best fit to the release data, and the release exponent value of 0.7260, lying between 0.45 and 0.89, is characteristic of non-Fickian (anomalous) transport, in which drug release is governed by a combination of diffusion through, and relaxation/erosion of, the swollen polymer matrix rather than by diffusion alone. This release behaviour is favourable for a topical antioxidant gel, as it suggests that the formulation would provide a sustained supply of active nanoparticles at the site of

application rather than an initial burst followed by rapid depletion.

Taken together, these results indicate that a Central Composite Design-based DOE approach successfully identified an optimum combination of cerium oxide nanoparticle and pomegranate peel extract concentrations that maximized both antioxidant activity and drug content of the nanoparticle suspension, and that the resulting nanoparticles — characterized by a small, narrowly distributed particle size, a highly positive zeta potential indicative of good colloidal stability, and confirmed crystallinity and thermal stability — could be successfully incorporated into a Carbopol 934 gel without loss of activity. The optimized gel combined skin-compatible pH, satisfactory rheological behaviour, excellent physical stability and a sustained, non-Fickian *in vitro* release profile, supporting its potential utility as a green-synthesized, biocompatible topical antioxidant system for applications such as the management of oxidative-stress-related skin disorders, photoprotection and wound healing.

CONCLUSION:

Cerium oxide nanoparticles were successfully synthesized by a green precipitation route using cerium nitrate hexahydrate and Punica granatum (pomegranate) peel extract as a natural reducing and stabilizing agent, and were statistically optimized with respect to nanoparticle and extract concentration using a Central Composite Design with antioxidant activity and drug content as responses. The design-optimized nanoparticle suspension (F2, and subsequently the optimized batch F14) exhibited high antioxidant activity and drug content, while the optimized nanoparticles themselves showed a nanoscale, narrowly distributed particle size (56.3 nm, PDI 0.213) and a highly positive zeta potential (+28.4 mV) indicative of good colloidal stability. Incorporation of the optimized nanoparticles into a Carbopol 934 gel yielded a stable, skin-compatible formulation with suitable pH (6.33 ± 0.02), viscosity (3278 ± 1.63 cP) and spreadability (6.7 ± 0.16 g·cm/s), together with sustained *in vitro* drug release (82.72 ± 0.05% at 8 hours) following non-Fickian, Korsmeyer–Peppas kinetics. Overall, the study demonstrates that a Design-of-Experiments-optimized, green-synthesized cerium oxide nanoparticle-loaded gel represents a safe, stable and effective topical antioxidant delivery system with promising potential for the management of oxidative-stress-related skin disorders and wound healing. In vivo antioxidant efficacy, skin permeation, dermal toxicity and long-term stability studies are recommended before clinical application.

REFERENCES:

1. Mohanraj VJ, Chen YJ. Nanoparticles – a review. Trop J Pharm Res. 2006;5(1):561-73.
2. Singh S, Pandey VK, Tewari RP, Agarwal V. Nanoparticle based drug delivery system: advantages and applications. Indian J Sci Technol. 2011;4(3):177-80.
3. Ealia SA, Saravanakumar MP. A review on the classification, characterisation, synthesis of nanoparticles and their application. IOP Conf Ser Mater Sci Eng. 2017;263(3):032019.
4. Bajaj KJ, Parab BS, Shidhaye SS. Nano-transethosomes: A novel tool for drug delivery through skin. Ind J Pharm Educ Res. 2021;55(1):1-10.
5. Kumari S, Sarkar L. A review on nanoparticles: structure, classification, synthesis & applications. J Sci Res. 2021;65(8):42-6.
6. Bani KS, Bhardwaj K. Topical drug delivery therapeutics, drug absorption and penetration enhancement techniques. J Drug Deliv Ther. 2021;11:105-10.
7. Ahmed M, Ali M. Semisolid dosage form: Topical gel formulation - a review. World J Pharm Res. 2016;5(12):1256-68.
8. Hussen NHA, Abdulla SK, Ali NM, Ahmed VA, Hasan AH, Qadir EE. Role of antioxidants in skin aging and the molecular mechanism of ROS: A comprehensive review. Asp Mol Med. 2025;5:100063.
9. Sowmya J, Gowda DV, Srivastava A. Topical gels: A recent approach for novel drug delivery. Int J Health Sci Res. 2015;5(10):305-12.
10. Dahle JT, Arai Y. Environmental geochemistry of cerium: applications and toxicology of cerium oxide nanoparticles. Int J Environ Res Public Health. 2015;12(2):1253-78.
11. Celardo I, Traversa E, Ghibelli L. Cerium oxide nanoparticles: a promise for applications in therapy. J Exp Ther Oncol. 2011;9(1):47-51.
12. Nyoka M, Choonara YE, Kumar P, Kondiah PP, Pillay V. Synthesis of cerium oxide nanoparticles using various methods: implications for biomedical applications. Nanomaterials. 2020;10(2):242.
13. Nadeem M, Khan R, Afridi K, Nadhman A, Ullah S, Faisal S, et al. Green synthesis of cerium oxide nanoparticles (CeO2 NPs) and their antimicrobial applications: a review. Int J Nanomedicine. 2020:5951-61.
14. Rajeshkumar S, Naik P. Synthesis and biomedical applications of cerium oxide nanoparticles – a review. Biotechnol Rep. 2018;17:1-5.
15. Ioannou ME, Pouroutzidou GK, Chatzimentor I, Tsamesidis I, Florini N, Tsiaoussis I, et al. Synthesis and characterization of cerium oxide nanoparticles: effect of cerium precursor to gelatin ratio. Appl Sci. 2023;13(4):2676.
16. Kim J, Hong G, Mazaleuskaya L, Hsu JC, Rosario-Berrios DN, Grosser T, et al. Ultrasmall antioxidant cerium oxide nanoparticles for regulation of acute

inflammation. ACS Appl Mater Interfaces. 2021;13(51):60852-64.
17. Turin-Moleavin IA, Fifere A, Lungoci AL, Rosca I, Coroaba A, Peptanariu D, et al. *In vitro* and in vivo antioxidant activity of the new magnetic-cerium oxide nanoconjugates. Nanomaterials. 2019;9(11):1565.
18. Zhao R, Zhao C, Wan Y, Majid M, Abbas SQ, Wang Y. *In vitro* and in vivo evaluation of alginate hydrogel-based wound dressing loaded with green chemistry cerium oxide nanoparticles. Front Chem. 2023;11:1298808.
19. Williams III C, Chambers-Wilson R, Roy J, Kowalczewski C, Jockheck-Clark AR, Christy R, et al. Cerium (III) nitrate containing electrospun wound dressing for mitigating burn severity. Polymers. 2021;13(18):3174.
20. Hala M. Abdelmigid, Hussien NA, Alyamani AA, Morsi MM, AlSufyani NM, Kadi HA. Green synthesis of zinc oxide nanoparticles using pomegranate fruit peel and solid coffee grounds vs. chemical method of synthesis, with their biocompatibility and antibacterial properties investigation. Molecules. 2022;27(4):1236.
21. Mohammadi P, Yaghoobi M, Bahaghighat EK, Asjadi F. Hydrothermally synthesized bio-functional ceria nanoparticles using orange peel extract: optimization, characterization, and antibacterial and antioxidant properties. RSC Adv. 2024;14(27):19096-105.
22. Blindheim FH, Ruwoldt J. The effect of sample preparation techniques on lignin Fourier transform infrared spectroscopy. Polymers. 2023;15(13):1-14.
23. Sankar J, Suresh Kumar S. Synthesis and characterization of nano cerium oxide using hydrothermal technique. INCAS Bull. 2021;13(1):173-81.
24. Beg S, Swain S, Rahman M, Hasnain MS, Imam SS. Application of design of experiments (DoE) in pharmaceutical product and process optimization. Pharm QbD. 2019;5(2):43-6.